TEXTURE AND RECRYSTALLIZATION IN 7010 ALUMINIUM ALLOY THICK PLATE

J.C. Ehrström, R. Shahani, A. Reeves, P. Sainfort
Pechiney Centre de Recherches de Voreppe, BP27, 38340 Voreppe, France

Abstract

The texture and recrystallization of thick aluminium alloy plate has been studied on laboratory specimens deformed in plane strain compression (PSC). After hot deformation, the texture is typical of hot rolled aluminium: crystallographic orientations are distributed along the α and β fibres. Significant recrystallization takes place during solution treatment with almost no change in texture. A recrystallization mechanism is proposed, according to which deformation subgrains grow in dispersoid free zones. Upon reaching a critical size, the subgrains grow into the adjacent grains, thereby becoming recrystallized grains.

Introduction

Recrystallization and texture have a significant effect on the fracture toughness and anisotropy of 7000 aluminum alloy thick plate. The relationship between recrystallization and these properties is well documented (see, for example [1]).

However, few publications deal with the basic recrystallization mechanisms of hot rolled 7000 alloys [2-6], and very few examine the texture development in these materials [7]. In order to improve our understanding of the above phenomena, measurements of texture and the area fraction of recrystallized grains in hot deformed and solution treated samples have been made, combined with optical and transmission electron microscopy (TEM).

Experimental methods

Samples were cut from a direct-chill cast 7010 alloy rolling ingot, the composition of which is given in Table I, and homogenized for 30 hours at 474°C. The heating time was 12 hours.

Table I. Composition of the 7010 alloy

element	Zn	Mg	Cu	Zr	Fe	Si
wt%	6.1	2.6	1.6	0.11	0.09	0.06

Hot deformation was conducted in plane strain compression (PSC) using a high speed servohydraulic testing machine. Samples were deformed at a constant srain rate of 1 s^{-1} to a strain of 1.0 (58% reduction). Three deformation temperatures were used: 370, 400 and 440°C. The samples were water quenched immediatly after hot deformation; half of each sample was solution treated for 1 h at 470°C in an air furnace, the heating time being 4 hours.

Table II. Processing conditions and area fraction of recrystallized grains following solution treatment

deformation temperature	370°C	400°C	440°C
fraction recrystallized *	21.0	10.2	5.0

* 95% confidence interval: ± 1.5%

Texture measurements were carried out on electropolished specimens taken at mid-thickness from the PSC samples [8]. The {111}, {200} and {220} pole figures were measured up to a tilting angle of 80° using a Siemens D-500 texture goniometer. The incomplete pole figures were corrected for background and defocussing and the Orientation Distribution Function (ODF) was calculated by the Series Expansion Method (L_{max} = 22).

Image analysis coupled with an optical microscope was used to measure the area fraction of recrystallized grains. A total surface of 12 mm^2 was analysed at x50 magnification. The specimens were prepared by polishing and etching in chromic acid after a heat treatment of 8 h at 160°C. Recrystallized grains are not etched by this solution, whereas unrecrystallized grains appear dark due to etching of the substructure (see figure 1).

Results

Texture

Typical orientation distribution functions (ODFs) are given in figure 2. They are consistent with the ODFs obtained at mid-thickness or quarter-thickness positions in industrial thick plate. The texture can be roughly described as orientation concentrations about the α and β fibres. However, the orientation scatter about the ideal Brass {011}<211>, S {123}<634> and Copper {112}<111> orientations is very large. No new texture components are generated by the recrystallization during solution treatment. The β-fibres shown in figure 3 indicate that the distribution of rolling texture orientations does not change significantly during solution treatment.

Optical microscopy

The as-deformed structure is relatively difficult to examine by optical microscopy since the chromic acid etch requires a solution treatment and artificial ageing.

The typical microstructure of the solution treated material is shown in figure 1. One can observe 3 types of microstructure :

- Large white recrystallized grains formed during the solution treatment. At high magnification, some white zones bordering unrecrystallized grains contain large subgrains. In fact, the difference between these large subgrains and the recrystallized grains is based only on their relative sizes. As it seems that there is no discontinuity in the sizes of recrystallized grains and large subgrains, our definition of recrystallized grains is somewhat ambiguous.

- Dark elongated zones containing very fine subgrains and corresponding with the central regions of original cast grains.

- Light grey zones, corresponding also to unrecrystallized grains and showing little sign of recovery. We expect recovery during solution treatment to give a clear subgrain structure ; this point must be further investigated. Our observations seem to show more of these zones in samples deformed at higher temperature.

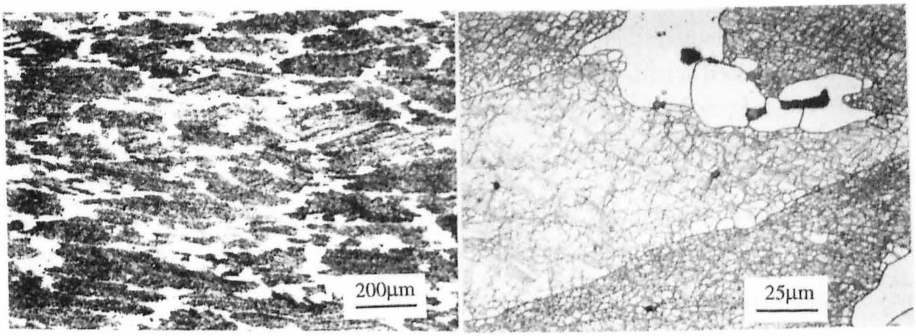

Figure 1. Microstructure of a solution treated sample (def. at 370°C, homo. 30 h 474°C).

TEM

The microstructure of as-deformed samples consists of fine (0.5-3 μm) subgrains with a high internal dislocation density.

Solution treatment results in much larger (1-5 μm), well-recovered subgrains. Figure 4 shows a large grain (diameter 20 μm) with a low dislocation density surrounded by smaller (1-3 μm) subgrains. The large grain is separated from the subgrains by high angle boundaries. Figure 5 shows one such high angle grain boundary, which has been pinned at several points by Al_3Zr dispersoids (cubic Pm3m, a=4.05 Å). The dispersoids close to the boundary within the large grain share the same orientation as those in the adjacent subgrain : {001}Al_3Zr // {001}subgrain, <100>Al_3Zr // <100>subgrain. This indicates that the high angle boundary has moved through a fixed array of dispersoids.

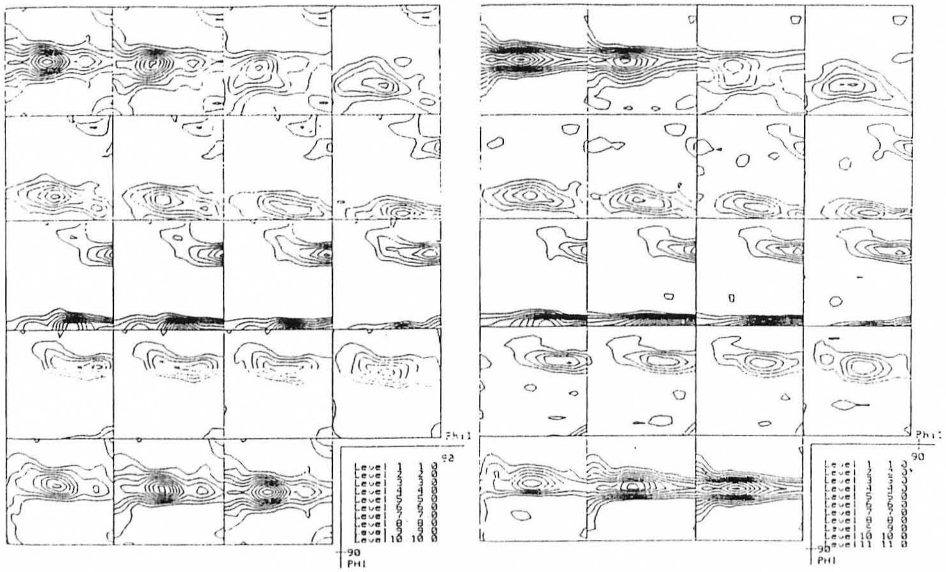

Figure 2. ODFs: as-deformed (left) and solution treated (right) (homo. at 474°C, def.400°C).

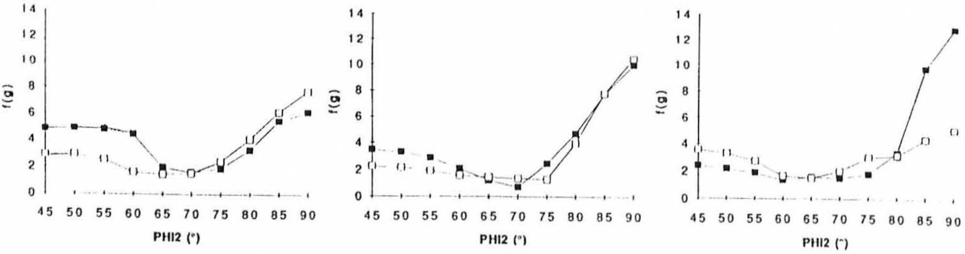

Figure 3. Comparison of intensities along the β-fibre before and after solution treatment following deformation at (a) 370°C, (b) 400°C and (c) 440°C.

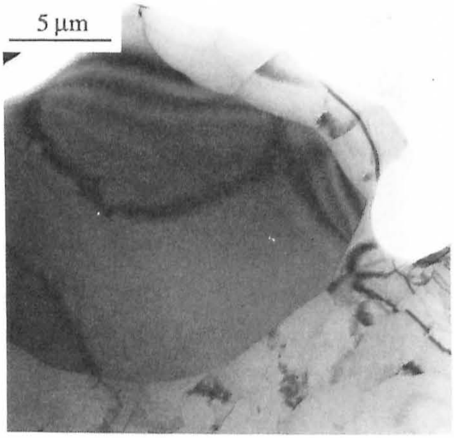

Figure 4. Bright-field TEM image showing a large grain surrounded by smaller subgrains (homogenization at 474°C, deformation at 440°C).

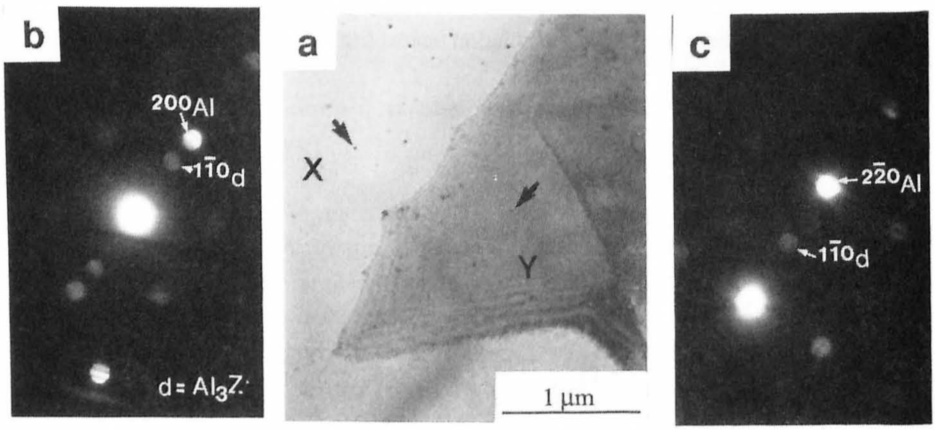

Figure 5. Bright field TEM image (a) showing pinning of a moving boundary by Al_3Zr dispersoids (homogenization at 474°C, deformation at 440°C). The large grain X to the left is oriented close to the [110]Al zone axis. The subgrain Y to the left has been tilted onto the [112]Al zone axis. Convergent beam diffraction patterns obtained from the arrowed dispersoids in the grain (b) and in the subgrain (c) show that they share the same orientation relationship: {001}Al_3Zr // {001}subgrain, <100>Al_3Zr // <100>subgrain.

Discussion

After hot deformation, the microstructure consists of large grains originating from the solidification structure, divided into fine subgrains. The Al_3Zr dispersoids keep the orientation of their surrounding matrix, which means that they rotate simultaneously during the deformation. The texture is typical of aluminum rolling textures.

The most striking observation is that the texture does not change significantly although significant recrystallization takes place during the solution treatment : the area fraction of recrystallized grains increases from about 0 to 5-20 % (Table II) with decreasing deformation temperature, and hence increasing stored energy.

Retained rolling textures after solution treatment could be produced by extended recovery or by large-scale strain induced boundary migration [9]. However, the micrographs indicate that recrystallization proceeds by a process of accelerated recovery in the grain boundary regions (giving large subgrains) followed by migration of the pre-existing grain boundaries. This high angle boundary migration is confirmed by the loss of the {001}Al_3Zr // {001}subgrain, <100>Al_3Zr // <100>subgrain orientation relationship. Recovery rates are expected to be higher near the grain boundaries since these regions are free of Al_3Zr dispersoids; the grain boundaries may also assist subgrain coalescence [10].

This mechanism requires a stored energy gradient to be built up across the grain boundary, either during deformation or through subsequent recovery. Note that some workers have reported that the Copper texture component is the first to recrystallize, whereas the Brass orientation is resistant to recrystallization, probably due to a low stored energy [11]. However, in this study the β-fibre is little changed by the partial recrystallization, indicating that the high angle boundary migration is not favoured by a particular texture component. The large eutectic particles present at or near the grain boundaries may assist in the nucleation process [12], but conventional particle stimulated nucleation of recrystallization does not appear to be the dominant mechanism, as this should result in a weakening of the rolling texture during solution treatment.

Conclusion

- The recrystallization is largely dependent on the hot deformation temperature. It takes place during the solution treatment.
- The microstructure of unrecrystallized grains can be classified into two types. One corresponds to a conventional recovered microstructure; the second has no apparent

subgrains, and needs to be further studied. This second type is mainly present after high temperature deformation.

- The texture of as-deformed samples is typical of aluminium alloys : orientations are distributed along the α and β fibres, with a large spread about the ideal Brass, S and Copper orientations.
- The texture of solution treated samples is essentially identical to the texture of as-deformed samples.
- The recrystallization mechanism is described as Strain Induced Boundary Migration following large subgrain growth in grain boundary regions.

Acknowledgements

The help of the McGILL University (P. Blandford and J.A. Szpunar) in the texture measurement and analysis is gratefully acknowledged.

References

1. J.T. Staley, in Properties Related to Fracture Toughness, ASTM STP 605, (1976), 71.

2. O.A. Alarcon, A.M. Nazar and W.A. Monteiro, "In Situ Recrystallization by Transmission Electron Microscopy of 7050 Aluminum Alloy" (Report INIS-BR-2364, 1990).

3. H. Suzuki, M. Kanno and H. Saito, J. Jpn Inst. Light Met. 36, (1986), 22.

4. K. Ranganathan, H.R. Last and T.H. Sanders, 3rd Conference on Aluminum Alloys, Trondheim 22-26 June 1992, (NTH-SINTEF, 1992), 15.

5. K. Ito and N. Nakashima, J. Jpn Inst. Light Met. 35, (1985), 147.

6. G. Itoh, B.L. Ou, H. Suzuki and M. Kanno, J. Jpn Inst. Light Met. 37, (1987), 587.

7. J. Liu, ASM/TMS Fall Meeting, Cincinnati 21-24 October 1991.

8. P. Blandford and J.A. Szpunar, Private Communication 1993.

9. E. Nes and W.B. Hutchinson, in Materials Architecture, ed. J.B. Bilde-Soerensen et al., RISØ National Lab., Roskilde, Denmark (1989), 233.

10. R.D. Doherty, in Recrystallization and Grain growth of Multi-Phase and Particle Containing Materials, ed. N. Hansen et al., RISØ National Lab., Roskilde, Denmark (1980), 57.

11. P.A. Hollinshead, Mater. Sci. Tech. 8, (1992), 57.

12. N. Hansen and B. Bay, Acta Met. 29 (1981), 65.